Simple target acquisition model based on $F\lambda/d$

Ronald Driggers,[a,*] Glenn Goranson,[b] Steve Butrimas,[b] Gerald Holst,[c] and Orges Furxhi[d]

[a]University of Arizona, Wyant College of Optical Sciences, Tucson, Arizona, United States
[b]University of Central Florida, Orlando, Florida, United States
[c]JCD Publishing Co., Oviedo, Florida, United States
[d]Imec USA Nanoelectronics Design Center, Kissimmee, Florida, United States

Abstract. The US Army Night Vision and Electronic Sensors Directorate's Night Vision Integrated Performance Model (NVIPM) is a robust, comprehensive, and sophisticated model that calculates the performance of an infrared imager in the task of target acquisition. The inputs are specifics about the target, atmosphere, optics, detector, electronics, and display and the outputs are probabilities of target detection, recognition, and identification. NVIPM is complicated and takes a good bit of time to master obtaining correct answers based on numerous assumptions and modeling experience. For midwave infrared (MWIR) and longwave infrared (LWIR) sensors, past research has shown that imaging system performance is strongly related to $F\lambda/d$, where F is the f-number, λ is the wavelength, and d is the detector pitch. $F\lambda/d$ provides a metric that relates how closely to diffraction-limited performance a sensor operates. We use the past $F\lambda/d$ work to develop a simple model that provides probability of target discrimination as a function of range that can be performed with a simple hand calculator or spreadsheet. We compare this model to the NVIPM calculations on 10 very disparate MWIR and LWIR sensors to show robust agreement. We also describe the conditions under which the simple model is valid.
 [DOI: 10.1117/1.OE.60.2.023104]

Keywords: Night Vision Integrated Performance Model; target acquisition; LWIR; MWIR; infrared imaging system.

Paper 20201416 received Nov. 30, 2020; accepted for publication Jan. 26, 2021; published online Feb. 23, 2021; corrected Mar. 11, 2021.

1 Introduction

There are several different military applications for infrared systems to include target acquisition, infrared search and track, infrared countermeasures, intelligence–surveillance–reconnaissance (ISR), and persistent ISR. Target acquisition is the largest of these military applications in that these sensors are on a wide variety of platforms to include dismounted soldiers (rifle sights), ground combat vehicles (tanks and armored personnel carriers), rotorcraft (helicopters), fighter jets, drones, and ships. Sometimes called targeting sensors, these sensors are the primary engagement sensor of a platform against targets.

Target acquisition sensors provide two functions. The first is search and detection. In the wide field-of-view (WFOV), the sensor scans the potential target area and "detects" both targets and clutter (nontargets). A detection occurs when the observer decides there is something there that warrants switching from WFOV to narrow field-of-view (NFOV) to interrogate an object. The object is deemed either a target or clutter and, if clutter, the observer goes back to the WFOV and continues the search process. Once in the NFOV, a discrimination task is conducted. There are various discrimination tasks as described in the literature[1–4] with several types of targets. One, in particular, is the 12-tank target set for tank discrimination (Fig. 1). The larger and more difficult the target set is, the harder it is to discriminate the targets (a difficulty measure known as V_{50} later in this paper). Other target parameters are contrast and target size, where both of these parameters make it easier or harder to discriminate the targets.

*Address all correspondence to Ronald Driggers, rdriggers@arizona.edu

0091-3286/2021/$28.00 © 2021 SPIE

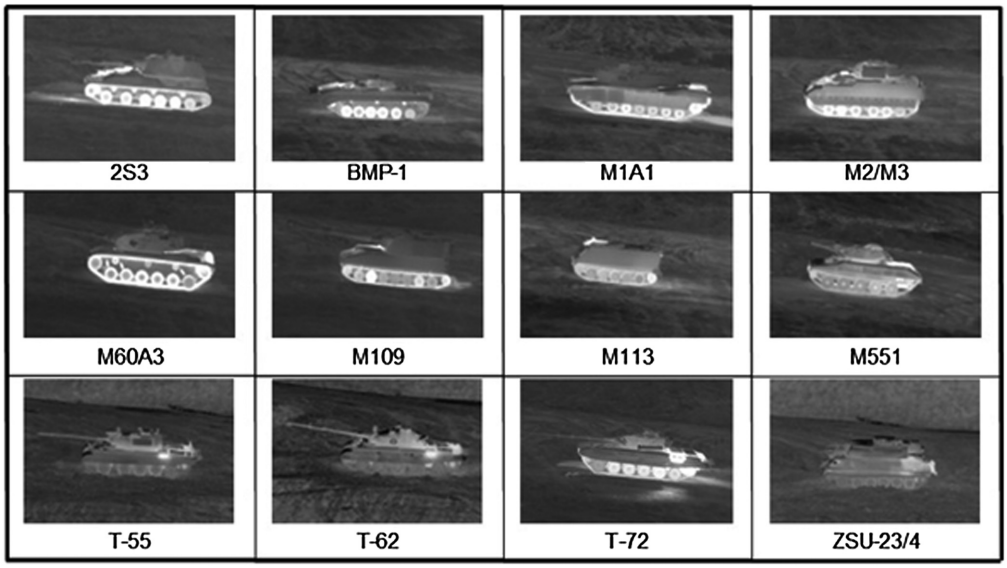

Fig. 1 Twelve tank identification training set.

Modeling the performance of infrared target acquisition sensors is described in more detail in Ratches' paper[5] and starts with Johnson fundamentals[6] and Schade's[7] treatment of resolution and sensitivity. A minimum resolvable temperature model was published by Ratches[8,9] in 1976 that began the performance prediction of infrared target acquisition systems. Several improvements including better noise treatment, two-dimensional geometries, increased resolution, and other aspects were published by D'Agostino et al. and Scott[10–12] and was known as FLIR90 and FLIR92. The ACQUIRE methodology allowed the conversion of these thermal imager performance models to provide field performance predictions.[13] These models provided for years of sensor analysis, design, and prediction capabilities until staring thermal imagers that were undersampled arrived. Vollmerhausen's[14,15] rework of the modeling approach to sensitivity and resolution [called the target task performance (TTP) metric or resulting in the NVTherm model], integration of eye limitations, and sampling theory provided a significant upgrade to the models that could support all thermal imagers as well as the integration of advanced signal and image processing techniques. Finally, Reynolds and Teaney[3,16,17] continued the improvement of the NVTherm model to standardize across all reflective and emissive imagers to account for different targets, various applications, and advanced image processing. The newest and latest model is still based on the TTP metric and is called Night Vision Integrated Performance Model (NVIPM).

NVIPM is a sophisticated model with more than 50 (and can have as many as a few hundred) input parameters and an output that provides probability of target discrimination as a function of range. It is the result of 50 years of research and development with years of anywhere from 3 to 10 research personnel working improvements. It provides accurate results for the defense industry, government labs, program offices, and analytical organizations. There are billions of dollars of target acquisition sensors developed every year based on the NVIPM model and accuracy is required when competition and stakes are high. The basic technical approach for NVIPM, the TTP metric, is described in Sec. 2. To become an expert in the use of the model and the trades necessary for analysis and design can take a significant investment in time and funding.

There is an easier way to provide probability of target discrimination as a function of range based on a relatively new metric called $F\lambda/d$, where F is the f-number, λ is the wavelength, and d is the detector pitch (we assume 100% fill factor). The approach is based on the metric developed by Fiete[18] and further developed by Holst.[19] This metric has already been used to analyze infrared detector size[20–22] and appears to provide good results if the metric is used within reasonable limitations. Our approach provides a simplified calculation that matches the results of NVIPM, but can be obtained using a simple hand-held calculator. The approach allows for a basic understanding of the resolution dynamics between optics and detector and provides good results for cases with good signal-to-noise ratio (SNR). This simple model is not appropriate for

sensors limited by random jitter effects, atmospheric turbulence, nor any advanced image processing algorithms. This model does provide the basic engineer with a rapid means for estimating thermal imager range performance for well-designed imagers.

2 NVIPM

NVIPM and its predecessors NVTherm, NVThermIP are based upon the same system contrast threshold function $\mathrm{CTF_{SYS}}$. However, the method to calculate the range is quite different. The contrast threshold function consists of an eye (observer) term and a noise term:

$$\mathrm{CTF_{SYS}} = \frac{\mathrm{CTF_{NAKED\,EYE}}}{\mathrm{MTF_{SYS}}}\sqrt{1+\left(\frac{\alpha\sigma_P(G)}{L_{\mathrm{AVE}}}\right)^2} \approx \frac{\mathrm{CTF_{NAKED\,EYE}}}{\mathrm{MTF_{SYS}}}\sqrt{1\ +k\left(\frac{1}{\mathrm{SNR}}\right)^2}. \quad (1)$$

$\mathrm{CTF_{NAKED\,EYE}}$ is Barten's human visual system (HVS) contrast model (evaluated with a nominal viewing distance). $\mathrm{MTF_{SYS}}$ is the product of all subsystem MTFs (limited here to optics, detector, and a flat panel display). The HVS provides tremendous spatial and temporal integration such that perceived SNR (PSNR) is much greater than the measured SNR. This integration is part of the complex noise term and is represented by the variable σ_P. The amount of perceived noise is a function of the sensor internal gain G. L_{AVE} is the display luminance. The experimentally derived constant α matches predicted values to experimental results. As a first-order approximation, the noise term is inversely related to the SNR. The noise term dominates for low signals (ΔT reduced by the atmospheric transmittance) and/or high noise (typically caused by atmospheric emission and/or noisy sensors).

Task difficulty (detection, recognition, and identification) is characterized by the N parameter in NVTherm and the V parameter in NVThermIP. NVIPM uses the same terminology, V. But with the major model changes, there is no relationship between the Vs, leading to some confusion. The 50% probability is labeled as N_{50} or V_{50}. Each target set and corresponding task difficulty have a unique N_{50} or V_{50}. Other probabilities are calculated using the empirically derived target transfer probability function (TTPF) (Table 1).

$$\mathrm{TTPF} = P = \frac{\left(\frac{X}{X_{50}}\right)^{\beta}}{1+\left(\frac{X}{X_{50}}\right)^{\beta}}, \quad (2)$$

where

$$\beta = A + B\frac{X}{X_{50}}.$$

NVTherm calculates range from the minimum resolvable temperature which is proportional to $\mathrm{CTF_{SYS}}$. The intersection of sensor $\mathrm{CTF_{SYS}}$ and the apparent target contrast is the limiting frequency (ξ_{CUT}). It is the highest frequency resolved at that particular contrast. With the ACQUIRE method, this limiting frequency, in cycles per milliradian, is converted to cycles on target by multiplying the limiting frequency by the target angular subtense (minimum dimension s divided by range R). It is noteworthy that s is a one-dimensional parameter. The number of

Table 1 TTPF parameters. Although both NVThermIP and NVIPM use V_{50} for $P = 50\%$, they are different values.

	Parameter X	A	B
NVTherm (2002)	N	2.7	0.7
NVThermIP (2006)	V	1.51	0.24
NVIPM (2013)	V	1.51	0

cycles on the target is compared to the N_{50}; an approach sometimes called the Johnson criterion. The ratio of cycles on target to N_{50} is the input to the TTPF. This process is repeated for various ranges and the probability is plotted as a function of range.

NVIPM and NVThermIP calculate range from the TTP. It provides a better range estimate for many thermal imagers to include staring systems. For mathematical convenience, the MTFs are considered separable:

$$\mathrm{TTP}_{\xi} = \int \sqrt{\frac{C_{\mathrm{DISPLAYED}}}{\mathrm{CTF}_{\mathrm{SYS}}(\xi)}}\, d\xi \;\; \mathrm{TTP}_{\eta} = \int \sqrt{\frac{C_{\mathrm{DISPLAYED}}}{\mathrm{CTF}_{\mathrm{SYS}}(\eta)}}\, d\eta. \tag{3}$$

The variables ξ and η are the horizontal and vertical spatial frequencies in cycles/milliradian. The constant, $C_{\mathrm{DISPLAYED}}$, is the observer's desired displayed contrast. It is not the apparent target contrast as used in NVTherm. To maintain a constant $C_{\mathrm{DISPLAYED}}$, the sensor gain increases as the apparent target contrast decreases. As indicated in Eq. (1), this gain affects the noise term. $C_{\mathrm{DISPLAYED}}$ is set to 0.2 as suggested by the NVIPM help manual. The TTP approach differs from the ACQUIRE approach in that the integration encompasses the system's resolution and sensitivity. The limits of integration start and end where the displayed target contrast intersects $\mathrm{CTF}_{\mathrm{SYS}}$. The area defined by the displayed contrast and $\mathrm{CTF}_{\mathrm{SYS}}$ is considered excess contrast. As the excess contrast increases, range increases.

For most sensors, $\mathrm{TTP}_{\xi} = \mathrm{TTP}_{\eta} = \mathrm{TTP}$. Then

$$V(R) = \frac{s}{R}\sqrt{\mathrm{TTP}_{\xi}\mathrm{TTP}_{v}} = \frac{s}{R}\mathrm{TTP}. \tag{4}$$

For NVIPM, the two-dimensional parameter s is the characteristic dimension. It is the square root of the target area in meters. Figure 2 compares the ACQUIRE and TTP approaches.

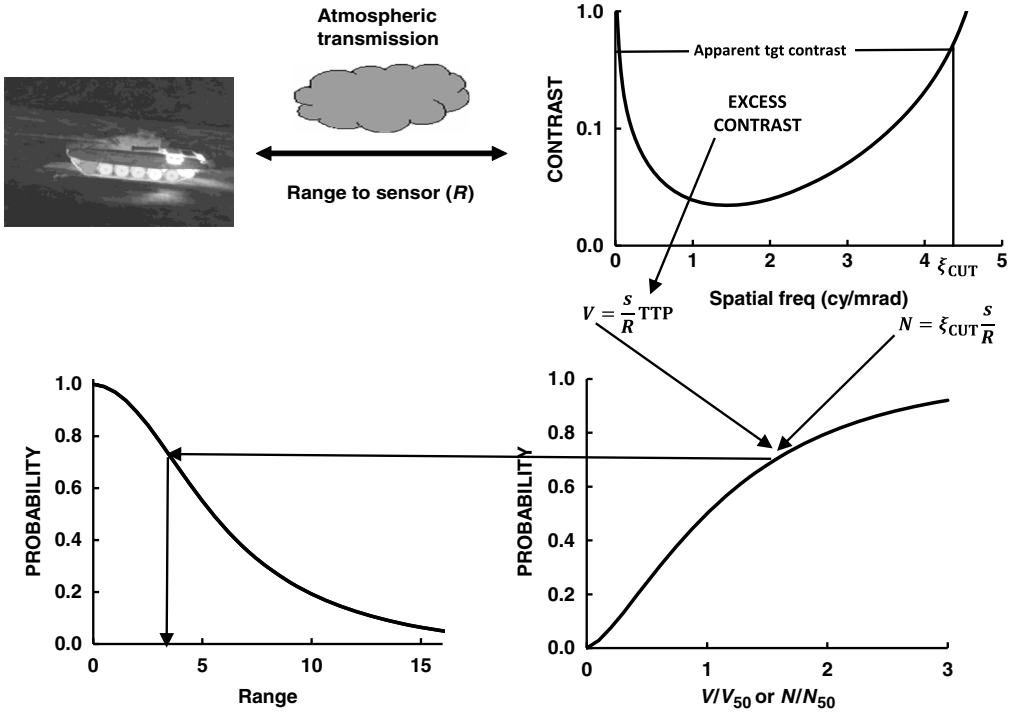

Fig. 2 ACQUIRE and TTP process. NVTherm calculates the range based upon the apparent contrast (target inherent contrast reduced by the atmospheric transmission). Whereas NVThemIP and NVIPM use the displayed contrast. For TTP, the lower limit of integration (not shown) is near zero and the upper limit is ξ_{CUT}. It is noteworthy that the apparent contrast varies with atmospheric transmission whereas $C_{\mathrm{DISPLAYED}}$ is a fixed value.

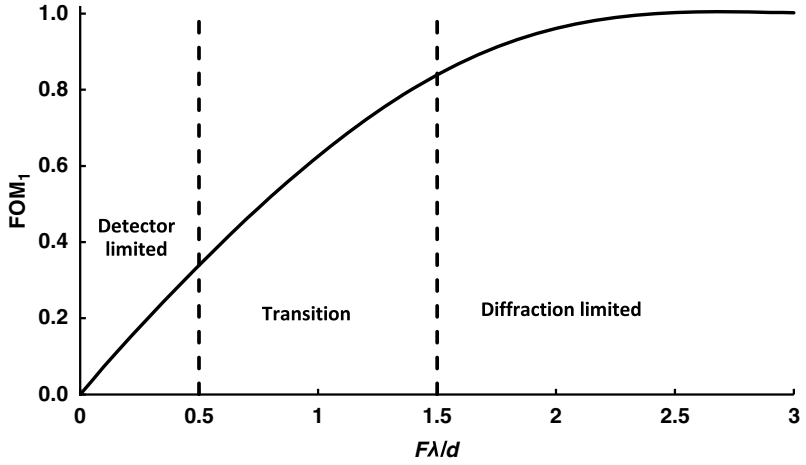

Fig. 3 FOM as a function of $F\lambda/d$ for a "bare bones" (optics, detector, and flat panel display) sensor. The vertical lines illustrate boundaries of detector-limited and diffraction-limited regions. The choice of 0.5 and 1.5 were arbitrary and the values selected are author dependent.

3 Simple Model Based on *Fλ/d*

Holst[19] derived a figure of merit (FOM) based on $F\lambda/d$ (Fig. 3):

$$\mathrm{FOM}_1 = -0.00247\left(\frac{F\lambda}{d}\right)^6 + 0.0261\left(\frac{F\lambda}{d}\right)^5 - 0.0901\left(\frac{F\lambda}{d}\right)^4 + 0.1098\left(\frac{F\lambda}{d}\right)^3 - 0.1582\left(\frac{F\lambda}{d}\right)^2 + 0.7402\left(\frac{F\lambda}{d}\right). \tag{5}$$

The wavelength is taken as the average of the cuton and cutoff wavelength, but in some cases, weighting the wavelength to the background temperature slightly increases the accuracy of the simple model. The FOM provides a nice trade between optical blur and detector blur and pitch for staring array imagers. Driggers and Holst[20,21] provided a two-dimensional design tool using $F\lambda/d$, where the range performance of diffraction-limited systems were traded with detector pitch, wavelength, and F-number.

The sixth-order polynomial is inconvenient for back of the envelope calculations. We considered two other approximations (Fig. 4):

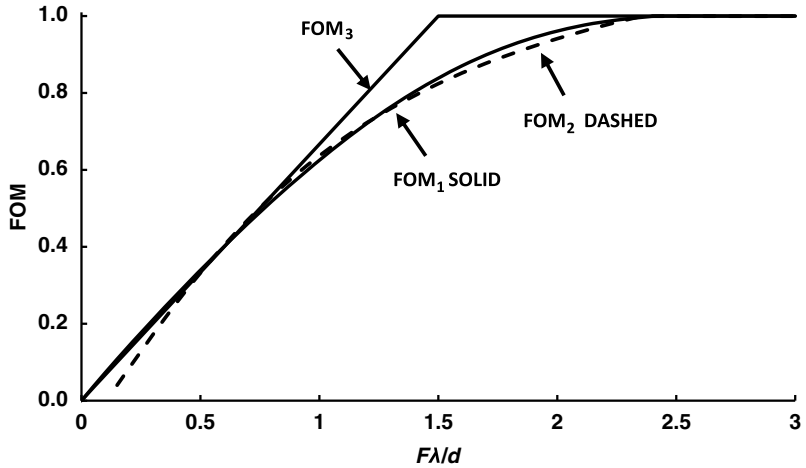

Fig. 4 Comparison of FOM_1, FOM_2, and FOM_3.

$$\mathrm{FOM}_2 = \mathrm{MIN}\left\{-0.05 + \frac{\mathrm{ATAN}\left(\frac{F\lambda}{d}\right)}{\mathrm{ATAN}(2)}, 1\right\} \quad \text{for} \quad \frac{\mathrm{ATAN}\left(\frac{F\lambda}{d}\right)}{\mathrm{ATAN}(2)} > 0.055, \tag{6}$$

$$\mathrm{FOM}_3 = \mathrm{MIN}\left\{\left(\frac{1}{1.5}\frac{F\lambda}{d}\right), 1\right\}. \tag{7}$$

Our simple range performance model is

$$R = \alpha\frac{D}{\lambda}\mathrm{FOM}, \tag{8}$$

where α is a calibration coefficient in meters that includes target discrimination complexity, target size, and desired probability (usually 70% or 90% in system specifications).

The piecewise linear model (FOM_3) is a worthwhile model from an understanding point of view in that when $F\lambda/d < 1.5$ (arbitrarily selected), Eq. (8) becomes $\frac{\alpha}{1.5}\frac{D}{\lambda}\frac{F\lambda}{d} = \frac{\alpha}{1.5}\frac{1}{\mathrm{IFOV}}$. The instantaneous field of view (IFOV) is the detector pitch divided by the focal length of the lens. In this detector-limited region, range increases as the IFOV decreases. When $F\lambda/d \geq 1.5$, Eq. (8) is $\alpha\frac{D}{\lambda}$ which is a diffraction-limited system. Here, range increases as the aperture increases or the wavelength decreases [suggesting an midwave infrared (MWIR) sensor over an longwave infrared (LWIR) sensor].

In this paper, we use FOM_2 and we calibrate α to provide a 50% probability (we will use this later to derive all probabilities). This is the basic simple model form that provides the range at which a 50% probability of target discrimination.

$$R_{50} = \alpha\frac{D}{\lambda}\mathrm{MIN}\left\{-0.05 + \frac{\mathrm{ATAN}(\frac{F\lambda}{d})}{\mathrm{ATAN}(2)}, 1\right\} \quad \text{for} \quad \frac{\mathrm{ATAN}\left(\frac{F\lambda}{d}\right)}{\mathrm{ATAN}(2)} > 0.055. \tag{9}$$

We also calibrate α to correspond to the standard 12 -tank target set.

4 Sensors

We selected a variety of available thermal imagers for comparison of the simple model to NVIPM calculations. The system sensitivity is expressed in terms of noise equivalent temperature difference (NETD) for microbolometers and a combination of well capacity and downstream noise for photon sensors with a well fill of 50%. The sensors are categorized by

Parameter	FLIR X8500sc SLS LWIR	FLIR X8500sc MWIR	DRS Zafiro® 640	FLIR Boson (scientific)	DRS Tamarisk	FLIR T1020 UCIR HDLWIR	6.6 Inch MWIR	12 Inch MWIR	11 Inch MWIR	5.5 Inch LWIR
	Commercial			μBolometers			Military			
Sensor Number	1	2	3	4	5	6	7	8	9	10
Aperture [mm]	40	40	68	24	54	31.3	169	301	280	141
Focal Length [mm]	100	100	272	24	65	36	1000	1875	1767	494
Pitch [μm]	12	12	12	12	17	17	15	15	15	12
Format	1280x1024	1024x1024	640x480	640 x 512	640x480	1024x768	640 x 512	1280x1024	1536x1024	640x480
Frame Rate (Hz)	180	60	120	60	30	30	60	60	60	60
Integration Time (ms)	5	16.67	7	16.67	16.67	16.67	16.67	10	16.67	16.67
Well Capacity (Me-)	11.5	7	7.7				7	5	7	12
Downstream Noise (e-)	3888	500	3500				500	500	500	500
NETD [mK]				40	50	20				
λ low [μm]	7.5	1.5	3.4	7.5	8	8	3.4	3.4	3	7.65
λ high [μm]	10.5	5	4.8	13.5	14	14	5.2	5.2	5	10.5
λ ave [μm]	9.0	3.3	4.1	10.5	11.0	11.0	4.3	4.3	4.0	9.1
Optical Transmission	0.8	0.8	0.8	0.8	0.8	0.8	0.8	0.72	0.8	0.8

Fig. 5 Key sensor parameters. This is only a partial list of input parameters required by NVIPM.

type and purpose ranging from commercial photon sensors to commercial microbolometers and military sensors (Fig. 5). This list spans different wavebands, fields of view, detection mechanism, and detector pitch and provides a diverse list to evaluate the simplified model. $F\lambda/d$ ranged from 0.68 (~detector limited) to 2.65 (diffraction limited).

The simple calculation of $F\lambda/d$ indicates systems that range from large detector pitch with small optical blur to long-range, diffraction-limited systems. Apertures range from inexpensive to high-performance military systems.

5 Prediction of R_{50}

We calculated the range at which a 50% probability of tank identification (R_{50}) using the simple model and NVIPM. We used Eq. (9) with an α calibrated to 0.538 m corresponding to a $V_{50} = 13$ cyc/mrad, a target characteristic dimension of 3.11 m, and a target contrast of 3 K. The results are provided in Table 2. In both cases, an atmospheric transmission of 0.85/km was used. The short-range sensors provided good agreement. The models appeared to diverge for the longer-range MWIR sensors as shown in Fig. 6. Figure 5 shows the errors for the longest range cases as significant. When the atmospheric transmission was changed from 0.85/km (average atmosphere) to 0.99/km (nearly transparent) for the three long-range cases, the errors for all 10 sensors averaged 1.4%.

As indicated in Eqs. (1), (3), and (4), as the SNR decreases, $\mathrm{CTF_{SYS}}$ increases, TTP decreases, and range decreases. The three cases that provided the significant errors occurred when the SNR dropped below 10 (target ΔT reduced by the atmospheric transmission divided by the NETD). When the real SNR was above 10, the results provided good agreement.

To understand the impact of reduced SNR on both the simple model and NVIPM, we varied the focal length and hence the f-number. As the focal length increased, the range increased. However, MWIR sensors become photon-starved resulting in a reduced SNR and a reduced range at high f-numbers. As stated previously, the NVIPM range prediction dropped compared to the simple model when the SNR decreased below 10. This low SNR is the case shown in

Table 2 Simple model R50 results compared to NVIPM results. Ranges provided in km.

	Name	$F\lambda/d$	D/λ	FOM	Predicted range	NVIPM	Error %
Sensor 1	FLIR X8500sc SLS LWIR	1.88	4444	0.93	2.22	2.25	1.0
Sensor 2	FLIR X8500sc MWIR	0.68	12,308	0.44	2.91	2.89	–1.0
Sensor 3	DRS Zaphiro MWIR	1.37	16,585	0.78	6.96	6.93	–0.4
Sensor 4	FLIR Boson	0.88	2286	0.56	0.69	0.69	0.2
Sensor 5	DRS Tamarisk 640 UCIR	0.78	4909	0.50	1.32	1.33	0.7
Sensor 6	FLIR T1020 UCIR	0.74	2845	0.48	0.73	0.75	1.9
Sensor 7	6.6-in. Aperture MWIR	1.70	39,302	0.89	18.82	17.31	–8.7
Sensor 8	12-in. Aperture MWIR	1.79	70,000	0.91	34.27	23.55	–45.5
Sensor 9	11-in. Aperture MWIR	1.81	65,116	0.92	32.23	24.01	–34.2
Sensor 10	5.5-in. Aperture MWIR	2.64	15,537	1	8.36	8.22	–1.7
Nearly transparent atmosphere ($\tau = 0.99$) —		—	—	—	—	—	—
Sensor 7	6.6-in. Aperture MWIR Easy Atm	1.70	39,302	0.89	18.82	18.35	–2.6
Sensor 8	12-in. Aperture MWIR Easy Atm	1.79	70,000	0.91	34.27	33.10	–3.5
Sensor 9	11-in. Aperture MWIR Easy Atm	1.81	65,116	0.92	32.23	31.77	–1.4

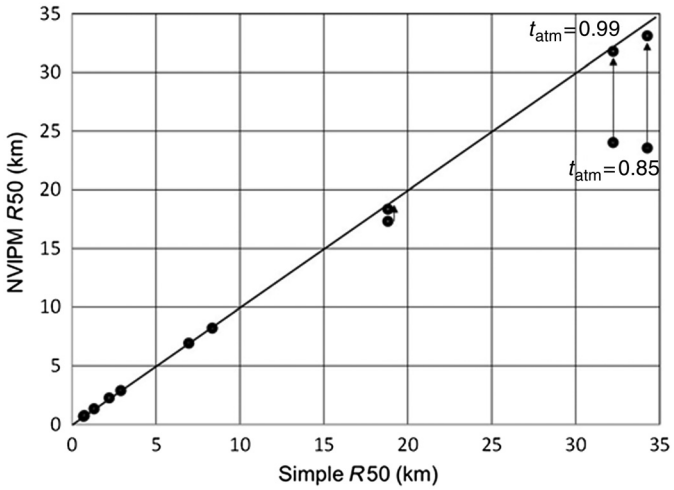

Fig. 6 NVIPM R_{50} results compared to the simple model R_{50} results. Sensors 4 and 6 appear as the same point (shortest range).

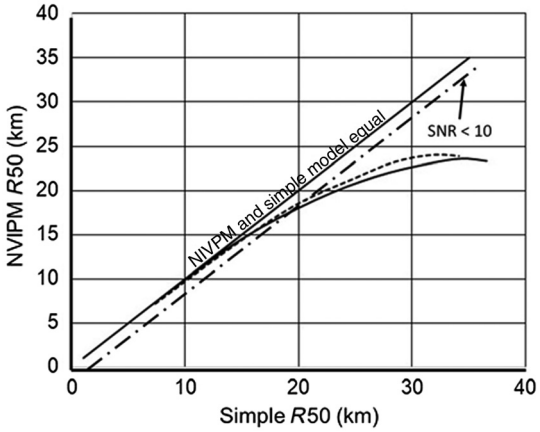

Fig. 7 Sensors 8 (dashed line) and 9 (solid line) with *f*-number (focal length) variation. The SNR <10 line shows where the simple model and NVIPM agree. Outside this limit, sensors 8 and 9 diverge from the NVIPM predictions.

Fig. 7, where the target contrast above the sensor CTF is becoming small and the integral for the TTP metric is signal starved.

In addition, both sensor 8 and 9 have frame rates of 60 Hz. With an eye integration time[23] of 0.15 s, meaning that 9 frames are integrated by the eye, the PSNR is $\sqrt{9}$ times the real-single frame SNR of 10, or a PSNR of 30 is required for the simple model to be valid.

$$\mathrm{PSNR} = \frac{\Delta T}{\mathrm{NETD}} T_{\mathrm{ATM}}(R) \sqrt{\mathrm{FR}\ \tau_{\mathrm{EYE}}} > 30, \tag{10}$$

where ΔT is the target contrast in Kelvin, NETD is the NETD of the sensor, FR is the frame rate of the sensor in frames per second or Hz, and τ_{EYE} is the eye integration time. $T_{\mathrm{ATM}}(R)$ is the atmospheric transmission over range R. Beer's law can estimate $T_{\mathrm{ATM}}(R)$ as $\tau_{1\ \mathrm{km}}^{R}$, where $\tau_{1\ \mathrm{km}}$ is the atmospheric transmission over a 1-km path length. PSNR has to be checked for any range that the simple model is used.

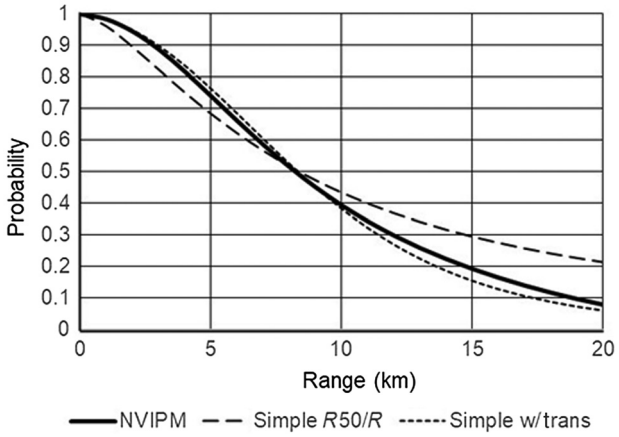

Fig. 8 Sensor 1 probabilities as a function of range.

6 Probability as a Function of Range

Equation (2) can be used to estimate probabilities at other ranges. It has been suggested that V/V_{50} is very similar to R_{50}/R. V_{50} can be viewed as a requirement for 50% probability of discrimination and a higher V provided by the sensor provides for a higher probability. In the same manner, R_{50} can be seen as a requirement for a 50% probability of discrimination, where a longer R provides for less information on target resulting in a lower probability of discrimination.

For the TTP version of Eq. (3), the default parameters in NVIPM for β is 1.51 with no V/V_{50} dependence in the exponent. If R_{50}/R is used to replace V/V_{50}, then a probability as a function of range can be generated and is shown as the "Simple $R50/R$" line in Fig. 8. The probability is not a very good match to the NVIPM range prediction (shown as the solid line). The reason is that the TTP metric, V, includes not only the resolution reduction associated with the range to the target, but it also includes the contrast reduction of the target which is also a function of range. To account for the contrast reduction (related to the root of available contrast to the system CTF), we rearrange Eq. (2) to

$$P(R) = \frac{\left(\sqrt{\frac{T_{\mathrm{ATM}}(R)}{T_{\mathrm{ATM}}(R_{50})}}\frac{R_{50}}{R}\right)^{\beta}}{1+\left(\sqrt{\frac{T_{\mathrm{ATM}}(R)}{T_{\mathrm{ATM}}(R_{50})}}\frac{R_{50}}{R}\right)^{\beta}}, \tag{11}$$

where $T_{\mathrm{ATM}}(R_{50})$ is the atmospheric transmission at range, $R50$. Now, Eq. (9) provides a reasonable approximation to NVIPM probabilities as a function of range with less than a 3% error for all probabilities greater than 50%. Very few systems are analyzed with probabilities lower than 50% or greater than 90%. Finally, for a Beer's law atmospheric transmission approximation, the term $T_{\mathrm{ATM}}(R)/T_{\mathrm{ATM}}(R_{50})$ can be replaced with $\tau_{1\,\mathrm{km}}^{R}/\tau_{1\,\mathrm{km}}^{R_{50}}$.

The Simple/w Trans (simple with transmission) range performance provides the contrast reduction action similar to that provided by the TTP metric. The difference here is that it is linear with the square root instead of the gradual function of the CTF bathtub shape. When the SNR becomes too low, the bathtub shape causes a divergence from the simple prediction from the NVIPM approach.

7 Characteristic Dimension and V_{50}

While we have shown that we can estimate infrared sensor range performance for a variety of sensors (within SNR limits) and for a variety of probabilities, what happens when the target set changes or the average target characteristic dimension changes? Target set discrimination difficulty, to include number of targets and how hard it is to discriminate the targets, is described by

V_{50}. A larger V_{50} provides for a more difficult target set and a smaller V_{50} provides for an easier target set. In addition, larger targets with larger characteristic dimension, d_{char}, are easier to discriminate and smaller targets are harder to discriminate. Now, Eq. (9) can be updated to

$$R_{50} = K\frac{d_{\text{char}}}{V_{50}}\frac{D}{\lambda}\text{MIN}\left\{-0.05 + \frac{\text{ATAN}(\frac{F\lambda}{d})}{\text{ATAN}(2)}, 1\right\} \quad \text{for} \quad \frac{\text{ATAN}(\frac{F\lambda}{d})}{\text{ATAN}(2)} > 0.055, \tag{12}$$

where K is determined from α to be 2.25 (unitless) for the current NVIPM theory (theory updated in 2013). For the NVIPM version 2013 and the later upgrades, Eq. (12) is valid for tracked vehicle identification. The current guidance on V_{50} and d_{char} for tracked vehicle identification are 13 cycles on target and 3.1 m, respectively. For tasks with a V_{50} greater than 10, Eq. (12) matches the current NVIPM model where the NVIPM help manual provides d_{char} and V_{50} for various tasks. Smaller V_{50}'s (less than 10) result in longer ranges and smaller target images on the display, where the current NVIPM theory changes include "apparent target angle" and "luminance dependent noise scaling," resulting in a nonlinear range dependency with $1/V_{50}$. For the legacy NVThermIP (2006 and 2009) models (which are still selectable as legacy components in the current NVIPM model), the range estimates are linear with $1/V_{50}$, but a $K = 4.05$ must be used. Also, the V_{50}'s and d_{char} for this earlier version of NVThemIP should be used for the target sets in Ref. 2 which provides V_{50} and d_{char} for various sets of targets, any target size, and for any LWIR or MWIR sensor for the SNR limitations described above. The simple model procedure is to determine the sensor parameters in f-number, wavelength, detector pitch, and aperture size. Then determine target set characteristic dimension and V_{50} difficulty criterion for the target set and calculate the R_{50}. Once the R_{50} is determined from Eq. (12), the probabilities as a function of range can be determined using the atmospheric transmission and Eq. (11).

8 Discussion

We now run the simple model described by Eqs. (11) and (12) for three different sensors (Fig. 5) for tracked target identification: a short-range LWIR (sensor 1), mid-range LWIR (sensor 10), and a long-range MWIR (sensor 9). In Fig. 9, the simple model results are plotted and compared to the NVIPM results. For the short-range and mid-range sensors, the models compare favorably. For the long-range MWIR (sensor 9), the simple model diverges from the NVIPM when the SNR reduces below the conditions of Eq. (10). When the NVIPM is run for the nearly transparent atmosphere case (transmission is 99% per 1-km path length), the SNR does not degrade, and the models agree. When using the simple model, the SNR estimates are important to determine whether the simple model can be used.

A few observations here are appropriate. The simple model can be used without Beer's law if the atmospheric transmission is known for the band as a function of range. Beer's law is

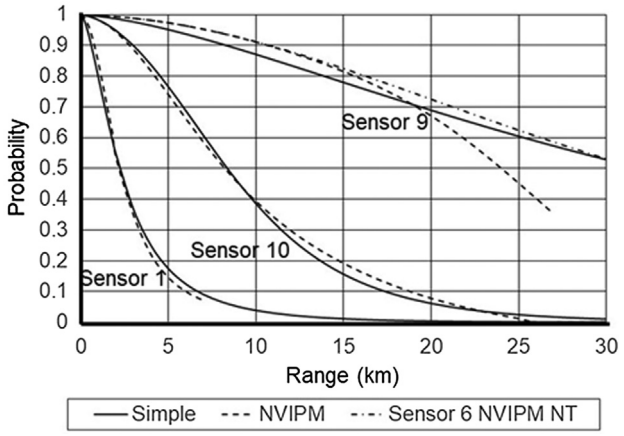

Fig. 9 Simple model compared to NVIPM. Simple model is solid lines, NVIPM is dashed lines, and NVIPM NT (nearly transparent) is the dash-dot line.

sometimes not a good approximation for the MWIR long range cases. Equations (11) and (12) can be used for different target sets (with V_{50}'s above 10) and characteristic dimensions with the limitations previously described. The simple model can be used for all target sets corresponding to NVThermIP 2006 and 2009 with $K = 4.05$ and V_{50}'s and d_{char} in Ref. 2. The simple model can be used easily for tracked target identification and other target sets with V_{50} of 10 and greater corresponding the current NVIPM.

The FOM_2 [Eq. (6)] is good for "bare bones" sensors that include optics, detector, and flat panel display. Other subsystem MTFs will reduce range and will require NVIPM. This simple model is not appropriate for sensors limited by random jitter effects, atmospheric turbulence, nor any image processing algorithms.

9 Conclusions

We have provided a simple sensor range performance prediction model based on $F\lambda/d$, where F is the f-number, λ is the wavelength, and d is the detector pitch. The model works well for basic infrared sensors and it can be applied to different target applications. The simple model was developed so that scientists, analysts, and engineers can predict range with a simple calculator. Future work on the simple model may be some simple relationship that predicts range for low SNR conditions.

References

1. R. G. Driggers et al., "Current infrared target acquisition approach for military sensor design and wargaming," *Proc. SPIE* **6207**, 620709 (2006).
2. R. G. Driggers, M. H. Friedman, and J. M. Nichols, *Introduction to Infrared and Electro-Optical Systems*, 2nd ed., Artech House (2012).
3. B. P. Teaney et al., "Human target acquisition performance," *Proc. SPIE* **8355**, 835510 (2012).
4. B. Teaney and J. Reynolds, "Next generation imager performance model," *Proc. SPIE* **7662**, 76620F (2010).
5. J. A. Ratches, R. H. Vollmerhausen, and R. G. Driggers, "Target acquisition performance modeling of infrared imaging systems: past, present, and future," *IEEE Sens. J.* **1**(1), 31–40 (2001).
6. J. Johnson, "Analysis of image forming systems," in *Proc. Image Intensifier Symp.*, pp. 249–273 (1958).
7. O. H. Schade, "Electro-optical characteristics of television systems," *RCA Rev.* **9**(1), 5–37 (1948).
8. J. A. Ratches et al., "*NVL static performance model for thermal viewing systems*," U.S. Electronics Command Rep. ECOM 7043, AD-A011 212 (1973).
9. J. A. Ratches, "Static performance model for thermal imaging systems," *Opt. Eng.* **15**(6), 156525 (1976).
10. J. A. D'Agostino et al., "*FLIR92 thermal imaging systems performance model analyst's reference guide*," Doc. UG5 008 993 USA CECOM Night Vision & Electron. Sensors Directorate, Fort Belvoir, Virginia (1993).
11. L. B. Scott and L. Condiff, "C2NVEO advanced FLIR systems performance model," *Proc. SPIE* **1309**, 168–180 (1990).
12. J. A. D'Agostino et al., "*FLIR92 thermal imaging systems performance model user's guide*," Doc. UG5 008 993 USA CECOM Night Vision & Electron. Sensors Directorate, Fort Belvoir, Virginia (1993).
13. J. A. D'Agostino et al., "*ACQUIRE range performance model for target acquisition systems version 1 user's guide*," U.S. CECOM Night Vision & Electron. Sensors Directorate Rep., Fort Belvoir, Virginia (1995).
14. R. H. Vollmerhausen et al., "*The targeting task performance (TTP) metric, a new model for predicting target acquisition performance*," NVESD Technical Report AMSEL-NV-TR-230, Fort Belvoir, Virginia (2005).

15. R. H. Vollmerhausen, E. L. Jacobs, and R. G. Driggers, "New metric for predicting target acquisition performance," *Opt. Eng.* **43**(11), 2806–13 (2004).
16. "NV-IPM users guide and help FILE [Computer Software]," US Army Night Vision and Electronics Directorate, Version 1.8 (2019).
17. B. P. Teaney and J. P. Reynolds, "Reflective band image generation in the night vision integrated performance model," *Proc. SPIE* **9820**, 982006 (2016)
18. R. D. Fiete, "Image quality and FN/ρ for remote sensing systems," *Opt. Eng.* **38**(7), 1229–1240 (1999).
19. G. Holst, "Imaging system performance based upon $F\lambda/d$," *Opt. Eng.* **46**, 103204 (2007).
20. R. G. Driggers et al., "Infrared detector size: how low should you go?" *Opt. Eng.* **51**(6), 063202 (2012).
21. G. C. Holst and R. G. Driggers, "Small detectors in infrared system design," *Opt. Eng.* **51**(9), 096401 (2012).
22. G. C. Holst, R. Driggers, and O. Furxhi, "Design considerations for advanced MWIR target acquisition systems," *Appl. Opt.* **59**, 4339–4348 (2020)
23. R. G. Driggers, R. H. Vollmerhausen, and K. A. Krapels, "Target identification performance as a function of temporal and fixed pattern noise," *Opt. Eng.* **40**(3), 443–447 (2001).

Biographies of the authors are not available.